Review

A Concise Review of Single-Molecule Magnets, Carbon Nanotubes and Hybrids Between Them

Mudasir A Yatoo[1*], Faiza Habib[2], Ahmad Husain[3], Sharique Ahmad[4] and Zubair Ahmad[5*]

[1] Imperial College London; m.yatoo15@imperial.ac.uk
[2] University College London; faiza.habib@ucl.ac.uk
[3] Indian Institute of Technology Ropar; ahmadhusain2065@gmail.com
[4] Aligarh Muslim University; shariqueahmad14@gmail.com
[5] Yeungnam University; zubair7157@yu.ac.kr
* Correspondence: m.yatoo15@imperial.ac.uk and zubair7157@yu.ac.kr

Abstract: Single-molecule magnets (SMMs) have garnered significant interest in the field of molecular magnetism due to their unique magnetic properties at the nanoscale. These molecular systems exhibit magnetisation behaviour reminiscent of conventional bulk magnets but with distinct advantages such as size-dependent properties and potential applications in quantum computing and high-density data storage. However, challenges remain in harnessing their properties for practical applications, including their susceptibility to degradation and limited control over their assembly and organisation.

In recent years, the integration of SMMs with carbon nanotubes (CNTs) has emerged as a promising strategy to address these challenges and unlock new possibilities for advanced magnetic materials. Carbon nanotubes, with their exceptional mechanical, electrical, and thermal properties, provide an ideal scaffold for the immobilisation and protection of SMMs, enhancing their stability and functionality. In this short review article, we provide a comprehensive review of the recent progress in the design, synthesis, characterisation, and applications of SMM-CNT hybrids.

Keywords: Molecular magnetism; single-molecule magnets; carbon nanotubes; single-molecule magnets-carbon nanotubes hybrids.

1. Introduction

Magnetochemistry is positioned on the interface between physics and chemistry. This discipline includes chemistry primarily as a source of new objects to which the molecular systems, such as linear, planar, or three-dimensional networking of certain entities, belong. It is mostly the chemistry of coordination compounds, which produces transition metal complexes having unpaired electrons as carriers of magnetic peculiarities. Under the effect of physical fields, these new materials display several noteworthy properties, with some ripe for technical utilisation. Therefore, the interdisciplinary appeal of magnetochemistry is enriched also by its output to material science. Contemporary research tendencies include the examination of molecular clusters, molecular magnets, spin-crossover systems, high-spin molecules as well as nanoscale magnetism.

Magnetic materials play vital roles in the daily lives of our race. Magnetism, first discovered by the ancient Greeks was used by the Chinese to create a "south-pointing" compass. Since the invention of the compass, the number of devices that use magnetic components has risen steeply. A few applications of magnetic materials include frictionless bearings, magnetic separators, loudspeakers, medical devices, data storage devices, microphones, switches, sensors, motors, and generators[1–5]. The wide-ranging commercial feasibility of magnetic materials has pushed research in this area.

 doi:10.20944/preprints202306.1276.v1

Conventional magnetic materials are two- and three-dimensional arrays of inorganic atoms, composed of transition metal or lanthanide metal containing spin units. These materials are usually produced at very high temperatures by using the methods of metallurgy. However molecular magnets are organic or inorganic/organic hybrid materials and comprised of either metal-containing spin units or organic radical-containing spin units[6]. Currently, the most promising and attractive field in molecular magnetism is the so-called SMMs. These systems are isolated molecules, usually with a large S in the ground state, and strong anisotropy.

2. Single Molecule Magnets

The single-molecule magnetic behaviour was recognised in the early 1990s with the cluster $[Mn_{12}O_{12}(AcO)_{16}(H_2O)_4]$, popularly known as $Mn_{12}Ac$ (Figure. 1)[7]. All the manganese centres in this cluster are octahedrally coordinated and they exhibit mixed valence: each Mn centre can be satisfactorily assigned a (+III) or a (+IV) oxidation state. The molecule may be termed as Class I — or valence localised by using the classification of Robin and Day. Or we say that it is reasonable to assign all the unpaired electrons to a particular Mn centre: they are regarded as localised with four electrons sitting in the outer shell of each of the eight Mn(III) ions and three electrons on each of the four Mn(IV) ions. In this cluster, the total spin ground state results from coupling interactions between pairs of these paramagnetic centres through the bridging oxide ions that hold the cluster together by a mechanism termed 'superexchange coupling'. The natural spin-pairing of electrons determines the nature of the interaction and thus, whether the interaction arranges the spins on the paramagnetic centres to be parallel, known as ferromagnetic coupling or antiparallel known as antiferromagnetic coupling, depends on geometric factors. In this Mn cluster, both types of coupling occur which leads to a total spin S = 10.

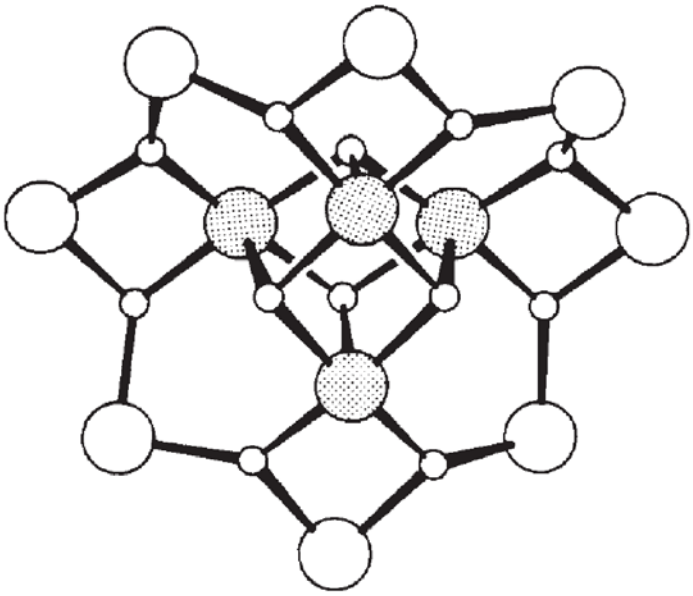

Figure 1. Schematic view of the core of Mn_{12} cluster. The largest white circle represents the manganese (III), S = 2, ions, the shaded circles represent the manganese (IV), S = 3/2, and the bridging oxides are represented by small white circles. For clarity, 16 acetate-bridging ligands and the four water molecules have been omitted. (reproduced from reference 7)

Preprints (www.preprints.org) | NOT PEER-REVIEWED | Posted: 19 June 2023 doi:10.20944/preprints202306.1276.v1

The magnetisation data for $Mn_{12}Ac$ shows a spin ground state S = 10, which is exposed to large negative zero-field splitting. The outcome of this is an energy barrier Ueff, separating the two lowest energy levels of Ms = -10 and Ms = +10. As a result of the energy barrier intrinsic to its ground state, the magnetisation of $Mn_{12}Ac$ can be pinned along one direction (easy axis) and then relaxes only slowly at very low temperatures. This type of multinuclear metal cluster that shows stable magnetisation of purely molecular origin is popularly known as SMM. The slow relaxation is also observed by hysteresis experienced when magnetisation is measured in a magnetic field sweep: on lowering the magnetic field again after reaching the maximum magnetisation, the magnetisation remains at high levels, and it requires a reversed field to bring magnetisation back to zero. Steps can be observed at regular intervals in the hysteresis loop, which correspond to an increase in the rate of change in magnetisation when there is an energy coincidence of the levels on the opposite parts of the double-well potential. This phenomenon is due to quantum tunnelling (Figure 2)[8,9].

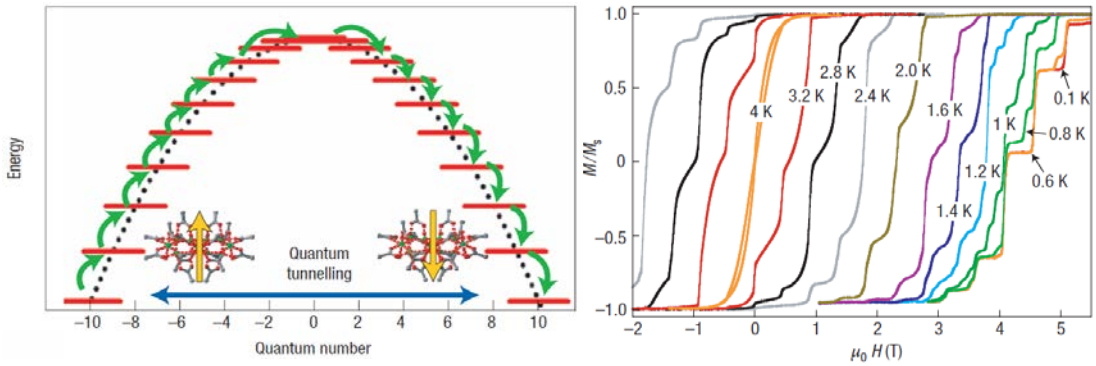

Figure 2. Dynamics of the magnetisation in SMMs. 2a, Schematic representation of the energy landscape of a SMM with a spin ground state S = 10. The magnetisation reversal can occur via quantum tunnelling between energy levels (blue arrow) when the energy levels in the two wells are in resonance. (reproduced from reference 8 and 9 respectively)

The magnetic behaviour of $Mn_{12}Ac$ comes from the combination of a non-zero spin ground state with a uniaxial anisotropy that when taken together creates a barrier stopping the inversion of the spin direction. As a consequence of this fact, its magnetisation undergoes slow relaxation below a blocking temperature, which is similar to what we observe in superparamagnetic systems, and thus a hysteresis can be recorded in these materials.

Since the discovery of this promising material, many compounds exhibiting similar kinds of behaviour have been reported. The vast majority of these consist of coordination clusters of 3d transition metals prepared by self-assembly processes where the structure of the final product has not been predicted. Most of this class of compounds features manganese ions with Mn III as the primary oxidation state. But over the years the search for new examples of such compounds has been extended to other metals like iron, nickel, vanadium, and cobalt of the 3rd row. A host of new approaches and synthetic procedures have been successfully developed and explored to prepare SMMs with novel and better properties.

SMMs possess an extensive range of functional properties like magnetic bistability, quantum tunnelling of magnetisation, and quantum coherence, which makes them unique materials. SMMs can be considered molecular equivalents of classical bulk ferromagnets. Therefore, it is likely to develop them for applications for storage purposes and processing of digital information. Novel applications of SMMs have also been predicted,

 doi:10.20944/preprints202306.1276.v1

including the use of molecular magnets (SMMs) in molecular spintronics and quantum computing[10,11].

In order to realise these highly useful applications of SMMs, there are a few challenges, which need to be solved. The foremost among them is that the unique properties of SMMs are currently realised only by using liquid helium cooling. Thus, we either need to raise the operating temperatures; blocking temperature in technical terms, significantly or some novel applications need to be discovered that temperature ceases to be an issue for harnessing these unique and novel applications. Another equally important challenge is that depositing and exploiting the functionality of individual SMM molecules on surfaces have been explored only with very few examples. There are many ways for depositing these materials for functional exploitation and carbon nanotubes with one macroscopic and two nanoscopic dimensions provide a perfect means to achieve this combination. However, care needs to be taken in achieving this coupling as SMM deposition on carbon nanotubes often leads to the decomposition of SMM and thereby devoid this molecule of its unique functionality[12,13]. Carbon nanotubes thus offer an excellent solution for using these SMMs for real-world applications. Furthermore, because of the superior electrical conductivity of carbon nanotubes, the functional state of SMM in such a hybrid can be controlled.

3. Carbon Nanotubes

Carbon nanotubes have got excellent properties and thus are being explored by a vast number of research groups around the globe for exploiting these properties. Carbon nanotubes (CNTs) were discovered as an electron microscopic prodigy in 1991 by Japanese researcher Sumio Iijima[14]. Iijima's discovery of multi-walled carbon nanotubes in the insoluble material of arc-burned graphite rods and independent forecast by Mintmire, Dunlap, and White that if single-walled carbon nanotubes could be made, then they would exhibit remarkable conducting properties helped generate the thrill among global physicists and chemists that is now associated with carbon nanotubes[15]. Nanotube research was further expanded greatly following the independent discoveries by Bethune *et al.* at IBM and Iijima at NEC of single-walled carbon nanotubes[16,17]. They further described the methods to specifically produce single-walled carbon nanotubes by adding transition-metal catalysts to the carbon in an arc discharge.

Since then, there has been intense activity related to the synthesis, structure, properties and applications of CNTs. The discovery of CNTs has triggered much research on other one-dimensional nano-objects such as inorganic nanotubes and nanowires.

Diamond and graphite are the two most common forms of crystalline carbon. Diamond has four-coordinate sp^3 carbon atoms which form an extended three-dimensional network whereas graphite has three-coordinate sp^2 carbons forming planar sheets. Fullerenes, which are relatively new allotropy, are closed-cage carbon molecules with three-coordinate carbon atoms. They present spherical or nearly spherical surfaces with C_{60} as a typical example. C_{60} shows a truncated icosahedral structure formed by twelve pentagonal rings and twenty hexagonal rings. It was the investigations led by Kroto *et al.* into the nature of carbon found in interstellar spaces that led to the discovery of fullerenes[18]. Fullerene has three-coordinate sp^2 carbons, but it is slightly pyramidalised, and not planar. This is because of some sp^3 characters present in the essentially sp^2 carbons. The key feature of this particular allotrope is the occurrence of five-membered rings in the structure, which provides the curvature necessary to form a closed-cage structure. In 1990, Kratschmer *et al.* found that the soot produced by arcing graphite electrodes contained C_{60} and other fullerenes[19]. Because of the relatively simple apparatus used to produce fullerenes in the laboratory, there occurred an intense rise in the research activity on these molecules and thus caused a resurgence in the study of carbon. Iijima in 1991, while producing

 doi:10.20944/preprints202306.1276.v1

fullerenes observed that nanotubules of graphite were deposited on the negative electrode during the direct current arcing of graphite[14]. These nanotubes are concentric graphitic cylinders closed at both ends due to the presence of five-membered rings.

Nanotubes can be either single-walled or multi-walled. Multi-walled nanotubes (MWNTs) contain a central tubule of nanometric diameter surrounded by graphitic layers separated by about 3.4 A°. This can be observed below in Figure 3[20].

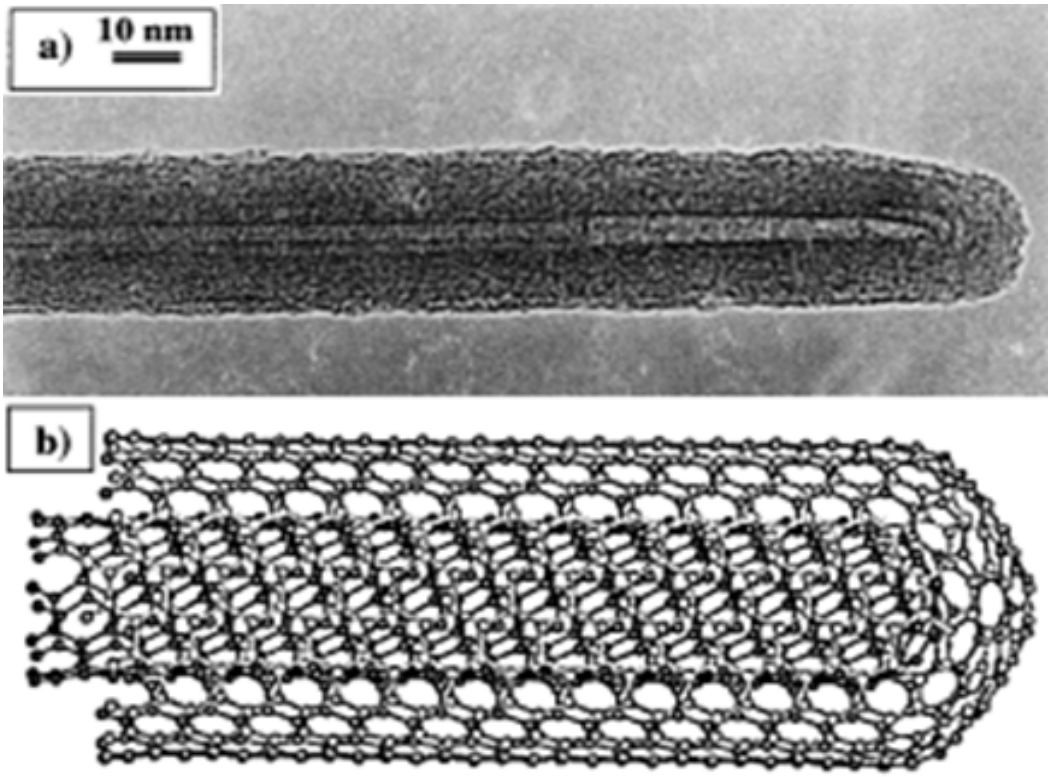

Figure 3. A transmission electron microscope (TEM) image of a MWNT is shown in Figure 3a. In this nanotube, graphite layers surrounding the central tubule can be seen. Figure 3b shows the structure of a nanotube formed by two concentric graphitic cylinders, obtained by force field calculations. (reproduced from reference 28)

However single-walled nanotubes (SWNTs) are composed of only tubules and there are no graphitic layers. Carbon nanotubes are the only form of carbon with extended bonding and yet with no dangling bonds. Since carbon nanotubes are derived from fullerenes, they are referred to as tubular fullerenes or bucky tubes.

Since the discovery of carbon nanotubes, several methods and techniques have been developed for preparing them. In addition to MWNTs, SWNTs have also been prepared in different ways[14,17]. Some important methods include electrochemical synthesis[21] and pyrolysis of precursor molecules[22]. Because of the fact of their versatility in future applications, the structural investigations of carbon nanotubes have been carried out extensively by high-resolution electron microscopy[23–26]. The carbon nanotubes, as prepared by arc vaporisation of graphite; are closed at either end, but can be opened by various oxidants[25,27]. Many research groups have extensively worked on filling some materials inside nanotubes and in fact, there has been considerable success in filling the nanotubes[28]. In addition to opening and filling, carbon nanotubes have also been doped with boron and nitrogen, thus giving rise to p-type and n-type materials respectively with dynamic properties.

 doi:10.20944/preprints202306.1276.v1

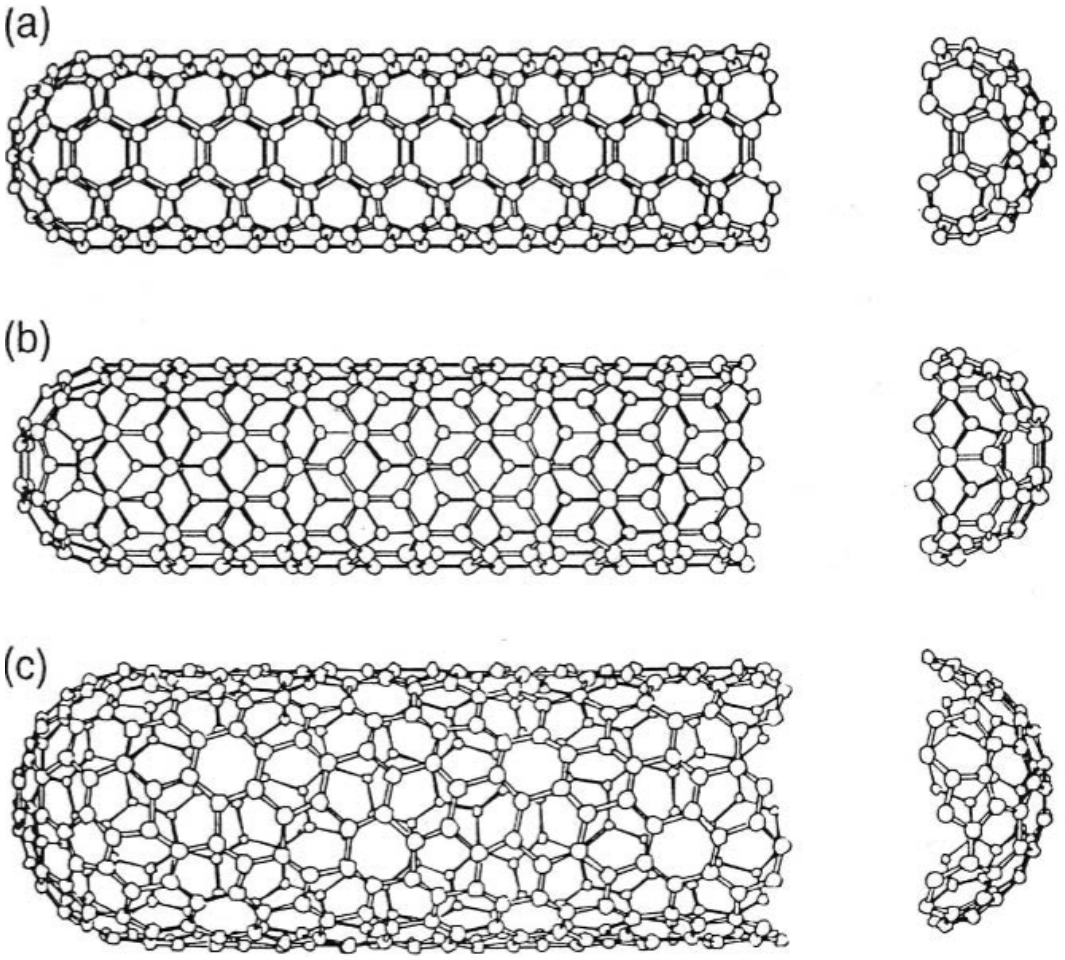

Figure 4. Models of (a) armchair, (b) zigzag, and (c) chiral nanotubes. (reproduced from reference 28)

Nanotubes, which are prepared by the arcing process usually, are found to consist of multi-layered, concentric cylinders of single graphene sheets when observed under a transmission electron microscope. The outermost tube diameter usually ranges from 10–30 nm as can be seen in Figure 3(a) but the diameter of the inner tubes is of the order of a only few nanometres. There occurs curling of a graphene sheet into a cylinder during the formation of nanotubes and thus helicity is introduced. This helicity, which has been confirmed by electron diffraction studies, suggests that the growth of nanotubes occurs as in the spiral growth of crystals. The separation between concentric cylinders in MWNTs is about 3.4 Å, which is close to the separation between the (002) planes of graphite. Usually, nanotubes are observed along their lengths, with the electron beam falling perpendicular to the axis of the nanotube under a transmission electron microscope. In high-resolution images, it is possible to see spots due to the lattice planes running along the length of the nanotubes. Ring-like patterns are found due to individual tubes involving cylindrical graphitic sheets, which are independently oriented with helical symmetry for the arrangement of the hexagons. Graphitic cylinders would have dangling bonds at the tips, but dome-shaped hemispherical fullerene-type units cap the carbon nanotubes. The capping units consist of pentagons to provide the curvature necessary for closure. Ajayan *et al.*[17] studied the distribution of pentagons at the caps of carbon nanotubes, finding that the caps need not be conical or hemispherical, but can form skewed structures. Cutting the C_{60} structure across the middle and adding a cylinder of graphite of the same diameter will give a good visualisation of the simplest possible single-walled carbon nanotube. If C_{60} is bisected normal to a five-fold axis, an armchair tube is formed, and if it is bisected normal to a three-fold axis, a zigzag tube is formed. Armchair and zigzag tubes are non-

 doi:10.20944/preprints202306.1276.v1

chiral. In addition to these, a variety of chiral tubes can be formed with the screw axis along the axis of the tube. Figure 4 demonstrates the models of the three types of nanotubes produced by bisecting the C_{60} molecule and adding a cylinder of graphite[20]. Nanotubes can be defined by a chiral angle (theta) and a chiral vector C_h, given by Equation (1), where a_1 and a_2 are unit vectors in a 2D graphene lattice and n and m are integers:

$$\mathbf{C}_h = n\mathbf{a}_1 + m\mathbf{a}_2 \qquad \text{Eq. 1}$$

The vector Ch connects two crystallographically equivalent sites on a 2D graphene sheet, and the chiral angle is the angle it makes concerning the zigzag direction, Figure 5. Rolling up the graphene sheet in such a way that the two points connected by the chiral vector coincide to form a tube. Several possible chiral vectors can be specified by Eq. (1) in terms of pairs of integers (n, m). Many such pairs are shown in Figure 5[20] and each pair (n, m) defines a different way of rolling up the graphene sheet to form a carbon nanotube of certain chirality. The limiting cases are n ≠ 0, m = 0 (zigzag tube), and n = m ≠ 0, (armchair tube).

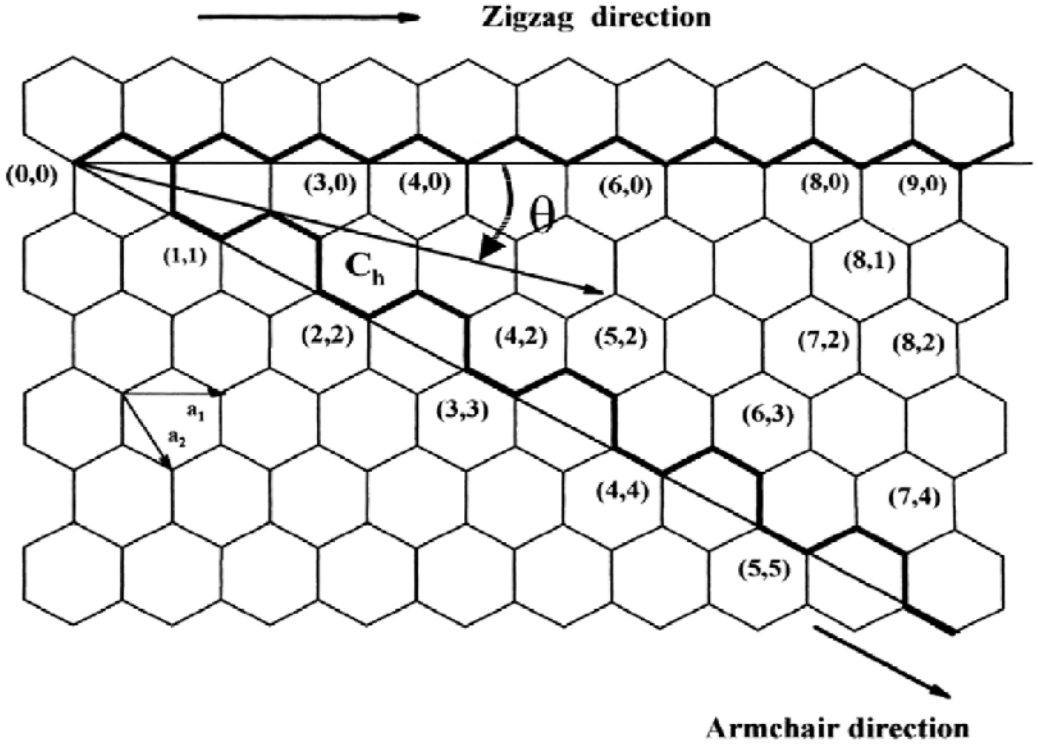

Figure 5. A 2D graphene sheet showing chiral vector Ch and chiral angle. (reproduced from reference 28)

Armchair SWNTs are metals; those with n - m = 3k, where k is a nonzero integer, are semiconductors with a very small band gap; and the rest are semiconductors with a band gap that inversely varies with the nanotube diameter[20,24]. The MWNTs consist of capped concentric cylinders separated by about 3.45A°, which is slightly larger than the interlayer spacing in graphite. This is because the number of carbon atoms increases as we go from an inner cylinder to an outer cylinder, and it is not possible to maintain perfect ABAB. . . . stacking as in graphite. Thus, an interlayer spacing close to that in turbostratic graphite is observed in MWNTs. In addition to pentagons and hexagons, carbon nanotubes can also have heptagons. Pentagons impart a positive curvature whereas heptagons give rise to a negative curvature to the otherwise flat graphene sheet made of hexagons. Thus, nanotubes with pentagons and heptagons will have unusual curvatures and shapes. Bent nanotubes arising from the presence of pentagons and heptagons on opposite sides of the tube have been observed[29]. Based on force field calculations, Tersoff and Ruoff suggest

 doi:10.20944/preprints202306.1276.v1

that the nanotubes will form cylindrical bundles in a crystal and large tubes will be hexagonal to maximise the van der Waals contact between the tubes[30]. Simulation studies indicate radial p-orbital character and large pyramidalisation angles at the sites of local deformation[31,32].

Since the discovery of carbon nanotubes, there has been immense interest in substituting carbon with other elements. Accordingly, boron–carbon (BaC), boron–carbon–nitrogen (BaCaN) and carbon–nitrogen (CaN) nanotubes have been prepared and characterised. Boron substitution in the carbon nanotubes gives rise to p-type doping and nitrogen-doped carbon nanotubes correspond to n-type doping. Novel electron transport properties are expected of such doped nanotubes[33].

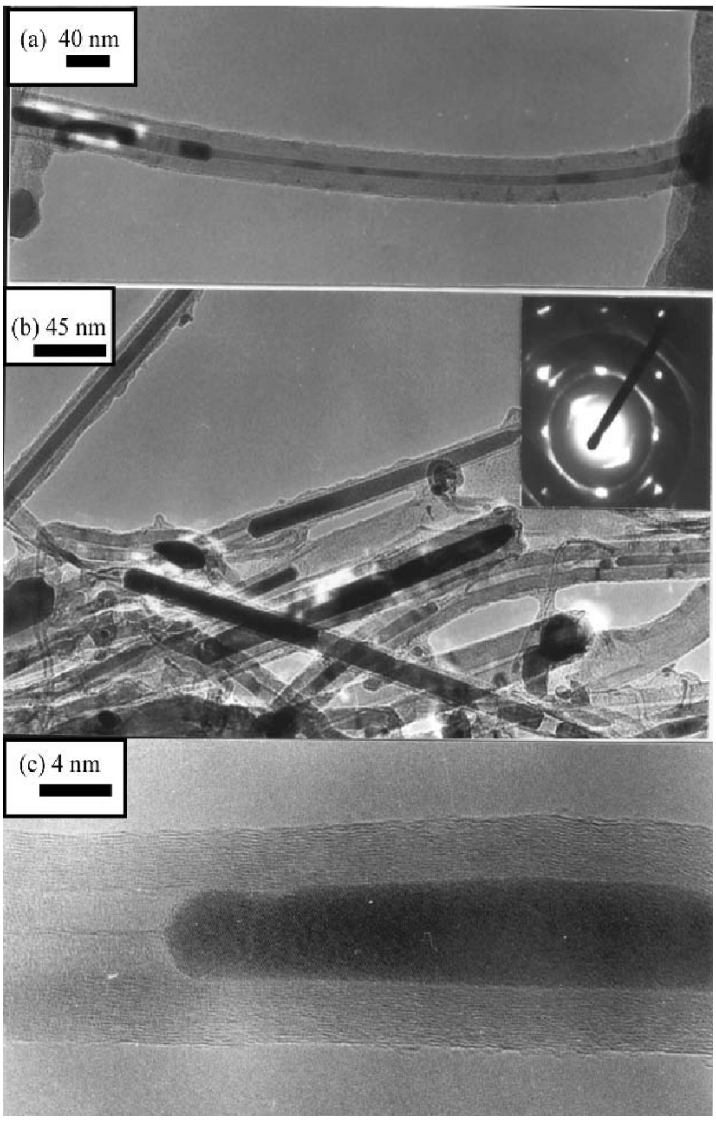

Figure 6. A. (a), (b) TEM images of the iron nanorods encapsulated inside the carbon nanotubes from aligned nanotube bundles. (c) HREM image of a single-crystal iron nanorod encapsulated inside a carbon nanotube. The inset in (b) represents the selected area electron diffraction (SAED) pattern of an iron nanorod. (reproduced from reference 34)

Furthermore, filling materials inside carbon nanotubes have been explored with great zeal. As can be seen in the TEM observations of aligned nanotubes produced by ferrocene + hydrocarbon pyrolysis. The presence of iron nanorods encapsulated inside the

 doi:10.20944/preprints202306.1276.v1

carbon nanotubes can be observed in the TEM images[34]. Typical TEM images of such nanorods are shown in Figure 6(a), (b) and (c). The inset in Figure 6(b) shows the selected area electron diffraction (SAED) pattern of the nanorods showing spots due to the (010) and (011) planes of Fe. In high-resolution electron microscopy (HREM) images shown in Figure 7[34], bundles consisting of 10–50 SWNTs forming highway junctions can be seen.

Multi-walled nanotubes are generally closed at either end, the closure is made possi-

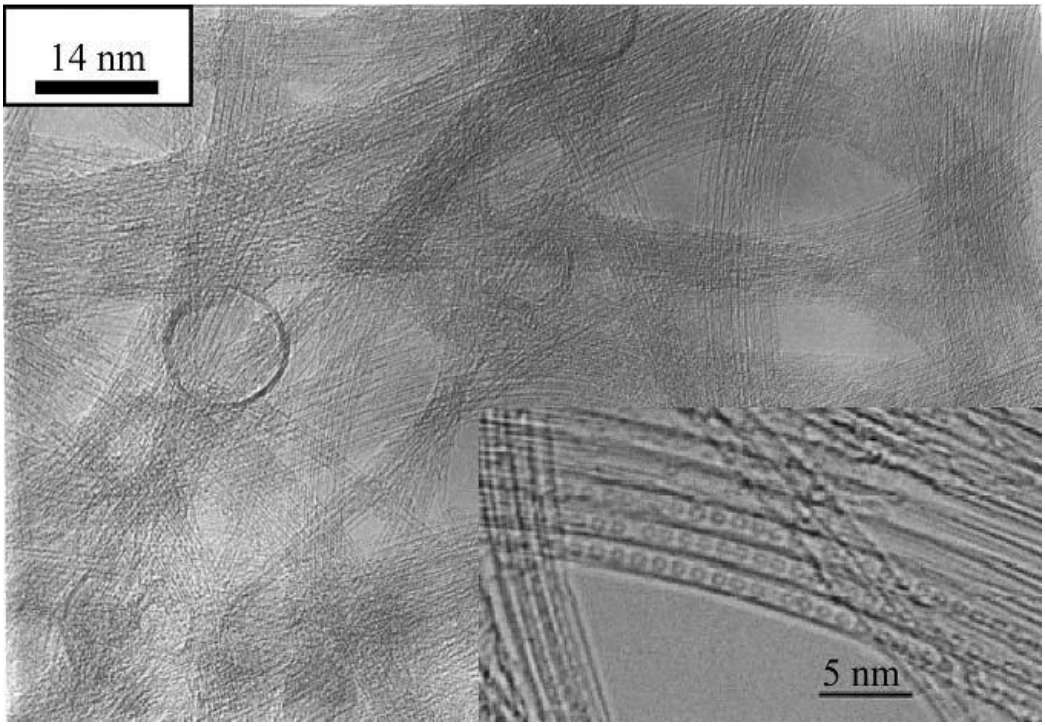

Figure 7. HREM image of SWNTs obtained by arcing graphite electrodes filled with Ni and Y_2O_3 under a He atmosphere (660 Torr). Inset: The HREM image of encapsulated fullerenes inside the SWNTs; scale bar is 5 nm. (reproduced from reference 34)

ble by the presence of five-membered rings. MWNTs can be uncapped by oxidation with carbon dioxide or oxygen at elevated temperatures[17]. High yields of uncapped MWNTs are, however, obtained by boiling them in concentrated HNO_3. Typical TEM images exhibit bamboo-shaped, nested cone-shaped cross sections as well as unusual morphology, including coiled nanotubes. Filling the opened nanotubes with metals has been accomplished. The well-known method involves the treatment of the nanotubes with boiling HNO_3 in the presence of metal salts such as $Ni(NO_3)_2$[35]. The nanotubes are opened by HNO_3 and filled with the metal salt. On drying and calcination, the metal salt transforms to the metal oxide and the reduction of the encapsulated oxide in hydrogen at around 400 °C gives rise to the metal inside the nanotubes. MWNTs have been opened by using a variety of oxidants and the opened nanotubes have been filled with Ag, Au, Pd, or Pt by different chemical means, rather than by reduction with hydrogen at high temperatures. By employing in situ techniques in a TEM, Bower *et al.* observed alkali metal intercalation into the SWNTs[36]. Sealed tube reactions of SWNTs and metal salts are also known to yield metal-intercalated SWNTs. To realise the conversion of sp^2 carbon of nanotubes into sp^3, Hsu *et al.* treated potassium intercalated MWNTs with CCl_4 hydrothermally and obtained crystallisation of KCl inside the nanotubes and within the tube walls[37]. Possible ways of closing the nanotubes, opened by oxidants, have been examined. Besides opening, filling and closing nanotubes, highly functionalised MWNTs have been prepared by treatment with acids. SWNTs are readily opened by mild treatment with acids and filled with metals. Acid-treated nanotube surfaces can be decorated by nanoparticles of metals such as Au, Ag or Pt.

 doi:10.20944/preprints202306.1276.v1

SWNT fragments were derivatised by Chen *et al.* with halogen and amine moieties so that SWNTs can be dissolved in organic solvents[38]. Furthermore, doping has been carried out to modify the electronic properties of SWNTs in the solution phase. Fluorination of SWNTs has been carried out by Mickelson *et al.*[39] Fluorinated nanotubes can be solvated in alcohol media and precipitated back by reaction with hydrazine. Scanning tunnelling microscope (STM) studies of fluorinated SWNTs reveal an interesting, banded structure followed by atomically resolved regions, indicating sidewall functionalisation. Starting from fluorinated SWNTs, Boul *et al.* have carried out alkylation by reaction with alkyl magnesium bromides or alky lithium[40,41]. Individual SWNTs have been deposited controllably on chemically functionalised nano-lithographic templates[42].

4. Single Molecule Magnets-Carbon Nanotube Hybrids

Since the discovery of single-molecule magnets (SMMs), there has been increasing interest in the development and exploration of polymetallic complexes of paramagnetic d-transition and lanthanide metals, which display SMM behaviour. For the d block, this class of molecules exhibit a magnetic bistability that is solely of the molecular origin and occurs from a combination of a high ground state electron spin (S), resulting from the magnetic exchange interactions between the individual ions within the cluster, and a large negative zero-field splitting, (D) within this ground state (Figure 10). The first known SMM is the dodecametallic, mixed-valence manganese cluster $[Mn_{12}O_{12}(O_2CMe)_{16}(H_2O)_4]$, ($Mn_{12}Ac$) which exhibits a ground state of S = 10 (Figure 11)[43,44]. Magnetic hysteresis in SMMs is observed at liquid helium temperatures. The temperature at which this retention of magnetisation is lost is defined as the blocking temperature, TB and is 4 K for $Mn_{12}Ac$. Therefore, if SMMs are to be utilised in areas such as data storage and quantum information processing, for example, SMMs need to be synthesised with higher blocking temperatures[45,46].

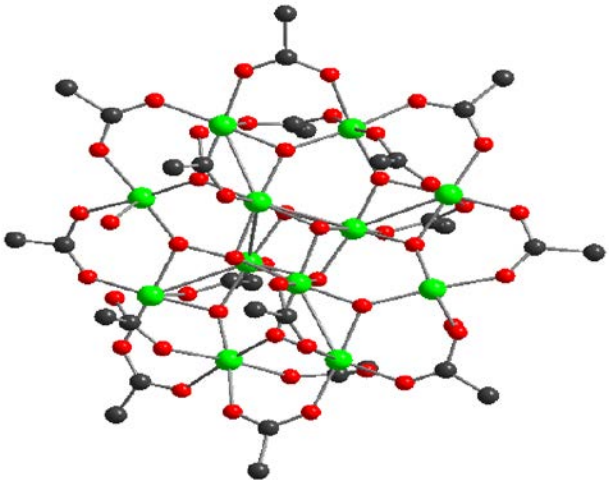

Figure 8. The Mn complex consisting of eight Mn(III), four Mn(IV), connected through bridging oxo-ligands, with sixteen acetates and four water ligands. (reproduced from reference 44)

Encapsulating SMMs in CNTs is one possible way of retaining SMM functionality with potentially higher blocking temperatures. CNTs are chemically and thermally very robust, which is highly advantageous for device fabrication. CNTs are also excellent electrical conductors[47]. Furthermore, in a CNT-SMMs hybrid, the nanotube that encapsulates the SMM also protects the guest molecule from the surrounding environs that would

Preprints (www.preprints.org) | NOT PEER-REVIEWED | Posted: 19 June 2023 doi:10.20944/preprints202306.1276.v1

otherwise induce strong decoherence, which is highly detrimental for quantum information processing applications[48].

Lapo Bogani *et al.* in 2009 reported the assembly of CNT–SMM hybrids using a tailor-made tetrairon(III) SMM, $[Fe_4(L)_2(dpm)_6]$ (dpm = dipivaloylmethane), designed to graft onto the walls of CNTs. The ligand L^{3-} (H_3L = 2-hydroxymethyl-2-(4- (pyren-1-yl)butoxy)methylpropane-1,3-diol), features an alkyl chain with a terminal pyrenyl group[49].

Extending their research results, they thus bridged the domains of molecular magnetism and CNTs by fabricating the first CNT–SMMs hybrids containing intact pyrene-functionalised SMMs in conditions compatible with the creation of electronic devices. Furthermore, their method enabled the controlled grafting of SMMs down to a single-molecule level and also demonstrated the single-SMM sensitivity of CNT–FETs (FETs = field-effect transistors). These results pave the way for the construction of "double-dot" molecular spintronic devices, where a controlled number of nanomagnets is coupled to an electronic nanodevice and the observation of the magneto-Coulomb effect.

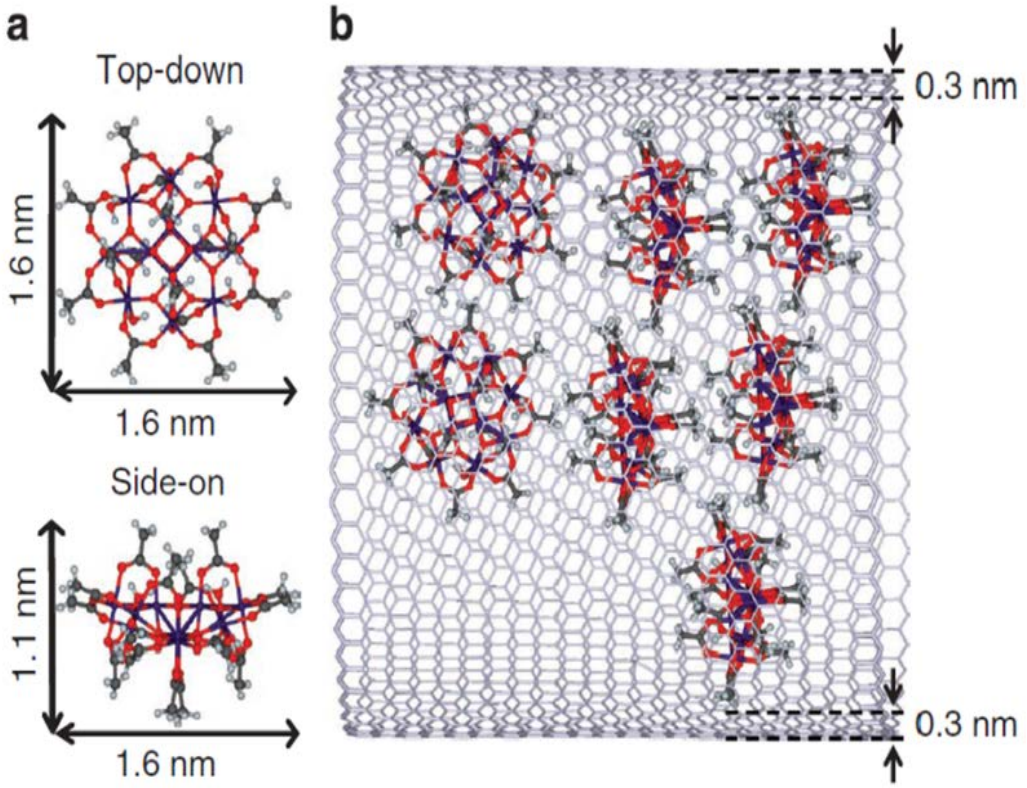

Figure 9. Chemical structure of $Mn_{12}Ac$ SMM and schematic representation of its encapsulation in a carbon nanotube. (a) Ball and stick structure of $Mn_{12}Ac$, with its dimensions indicated by double-headed arrows. Carbon, hydrogen, manganese and oxygen atoms are shown as grey, light-blue, purple and red circles, respectively. (b) Schematic representation of the innermost layer of a GMWNT hosting $Mn_{12}Ac$ molecules. (reproduced from reference 50)

Maria del Carmen *et al.* reported in 2011, the preparation and study of a hybrid material in which they encapsulated $Mn_{12}Ac$ inside MWNT (Figure 9)[50]. They further showed that the SMM functional properties of $Mn_{12}Ac$ are fully retained and that the molecules undergo a large degree of orientational ordering inside the nanotube. This ordering is

 doi:10.20944/preprints202306.1276.v1

beneficial for addressing purposes and for regulating the electronic properties of the nanotube.

They used supercritical CO_2 for the transport of the SMM molecules into the nanotubes. Supercritical CO_2 because of the small size of CO_2, its low viscosity, high diffusivity and zero surface tension is a good carrier fluid for the encapsulation of molecules, because it allows the guest molecule to penetrate the nanotubes without hindrance, enabling the insertion of the desired guest species with ease.

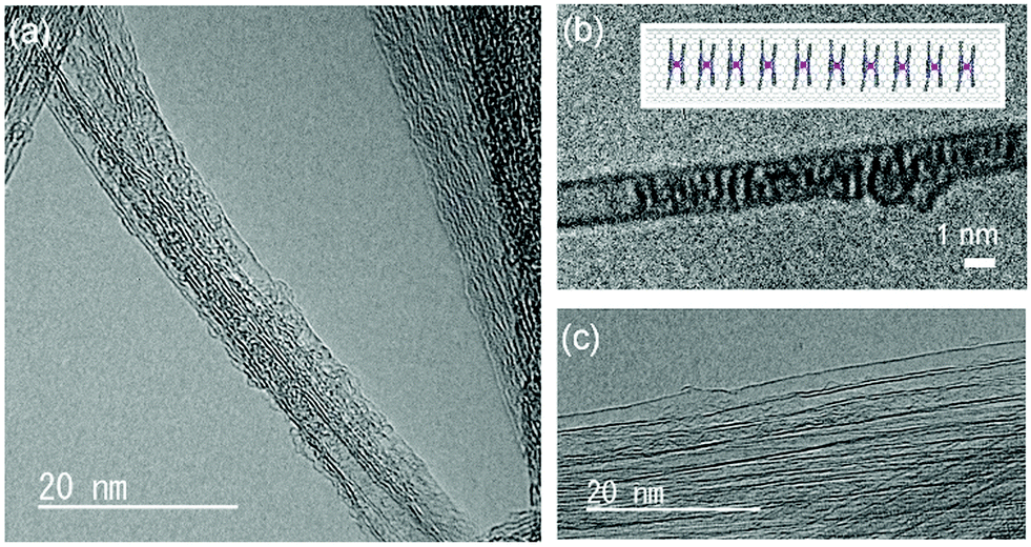

Figure 10. Structural characterization of TbPc2@SWCNT. Conventional bright field and phase contrast TEM images of TbPc2 encapsulated in SWCNTs. (a) TbPc2 was confirmed to be inside SWCNTs. Tb was detected by using EDX (see Fig. S3, ESI†). (b) TbPc2 were partially stacked one-dimensionally in SWCNTs. (c) Empty SWCNT. (reproduced from reference 52)

Yatoo *et al.* reported encapsulation of $Dy(acac)_3(H_2O)_2$ (acac = acetylacetonato) SMMs in the internal nanospace of MWCNTs by using a capillary method and later confirmed the encapsulation by TEM[51]. They further confirmed AC magnetic susceptibility measurements and observed both the in-phase and out-of-phase signals were clearly frequency dependent, indicating that $Dy(acac)_3(H_2O)_2$ complexes still exhibited SMM-like properties.

Katoh *et al.* reported the synthesis and characterisation of Terbium(iii) bis-phthalocyaninato ($TbPc_2$) SMM and single-walled carbon nanotube hybrids (Figure 10).[52] The frequency dependence due to $TbPc_2$ was shown by using ac magnetic susceptibility measurements and reported the activation energy barrier Ueff of 430 cm^{-1}, consistent with those of pristine $TbPc_2$. They further reported the electronic interactions between the $TbPc_2$ molecules and SWCNTs in these hybrids and showed bandgap modulation due to encapsulation, thereby opening up the possibility of their field effect transistor applications.

Yamashita and co-workers recently reported the encapsulation of a metallofullerene single-molecule magnet, Dy2ScN@C80, into SWCNTs (Figure 11)[53]. Interestingly they observed weakened SMM behaviour after encapsulation, in stark contrast to the Dy2ScN@C80 and ascribed the partial SMM functionality loss to either preferential orientation of $Dy_2ScN@C80$ in SWCNTs or charge transfer from Dy2ScN@C80 to SWCNTs.

Preprints (www.preprints.org) | NOT PEER-REVIEWED | Posted: 19 June 2023 doi:10.20944/preprints202306.1276.v1

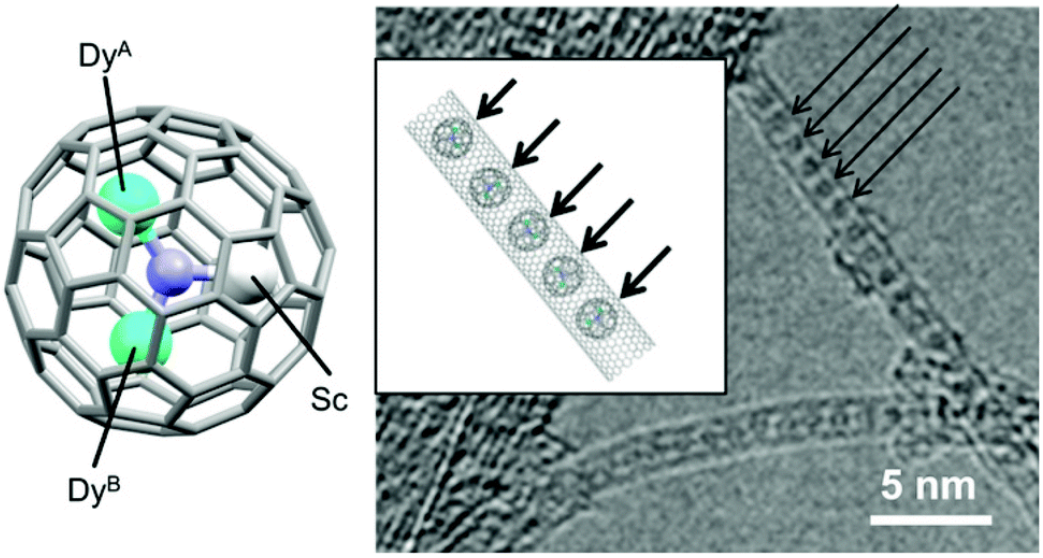

Figure 11. Molecular structure of Dy2 (left) and the high-resolution TEM image (right) of Dy2@SWCNT. The inset in the right-side figure is an illustration of Dy2@SWCNT. (reproduced from reference 53)

While there have been successful reports of synthesising SMM-CNT hybrids, the major challenge of obtaining improved SMM functionality still remains. Since there have been a few successful demonstrations of SMMs retaining their unique functionality when encapsulated in CNTs, the research direction appears on the right track. As a direction for future work, stacking of SMMs in a one-dimensional chain structure inside the CNTs might hold the key and allow for an increase in magnetic hysteresis and blocking temperature so that these materials could be realised for real-world applications.

5. Conclusions and Perspectives

Integrating single-molecule magnets (SMMs) with carbon nanotubes (CNTs) has demonstrated great potential in advancing the field of molecular magnetism and developing novel magnetic materials. The combination of SMMs and CNTs represents a compelling avenue for designing and fabricating advanced magnetic materials with tailored properties. The synergistic effects arising from this hybridisation open exciting opportunities for fundamental studies of molecular magnetism and the development of novel applications in nanotechnology.

The synergistic coupling between SMMs and CNTs in these hybrid systems offers a range of unique advantages. The exceptional mechanical, electrical, and thermal properties of CNTs provide an ideal scaffold for the immobilisation and organisation of SMMs, enabling precise control over their assembly and functionality. Moreover, hybridisation often leads to novel functionalities and improved performance, arising from the interactions between the magnetic moments of SMMs and the electronic structure of CNTs.

Despite the significant progress made in the synthesis, characterisation, and applications of SMM-CNT hybrids, several challenges and opportunities remain. Further research efforts are needed to improve the understanding of the fundamental interactions between SMMs and CNTs, optimise the design and synthesis of hybrid systems, and explore new strategies for tailoring their properties. Additionally, advancements in fabrication techniques and characterisation methods will enable the realisation of complex hybrid architectures and a deeper understanding of their structure-property relationships.

Funding: This research received no external funding.

Data Availability Statement: No new data were created or analysed in this study. Data sharing does not apply to this article.

Conflicts of Interest: The authors declare no conflict of interest.

References

(1) Leuenberger, M. N.; Loss, D. Quantum Computing in Molecular Magnets. *Nature 2001 410:6830* **2001**, *410* (6830), 789–793. https://doi.org/10.1038/35071024.

(2) Gatteschi, D.; Sessoli, R.; Sessoli, R.; Gatteschi, D. Quantum Tunneling of Magnetization and Related Phenomena in Molecular Materials. *Angewandte Chemie International Edition* **2003**, *42* (3), 268–297. https://doi.org/10.1002/ANIE.200390099.

(3) Rocha, A. R.; García-Suárez, V. M.; Bailey, S. W.; Lambert, C. J.; Ferrer, J.; Sanvito, S. Towards Molecular Spintronics. **2005**. https://doi.org/10.1038/nmat1349.

(4) Joachim, C.; Gimzewski[2], J. K.; Aviram[3], A. Electronics Using Hybrid-Molecular and Mono-Molecular Devices. *Nature* **2000**, *408*.

(5) Yatoo, M.; Cosquer, G.; Morimoto, M.; Irie, M.; Breedlove, B.; Yamashita, M. 1D Chains of Lanthanoid Ions and a Dithienylethene Ligand Showing Slow Relaxation of the Magnetization. *Magnetochemistry* **2016**, *2* (2), 21.

(6) Miller, J. S.; Epstein, A. J. Organic and Organometallic Molecular Magnetic Materials—Designer Magnets. *Angewandte Chemie International Edition in English* **1994**, *33* (4), 385–415. https://doi.org/10.1002/anie.199403851.

(7) Sessoli, R.; Gatteschi, D.; Caneschi, A.; Novak, M. A. Magnetic Bistability in a Metal-Ion Cluster. *Nature 1993 365:6442* **1993**, *365* (6442), 141–143. https://doi.org/10.1038/365141a0.

(8) Bogani, L.; Wernsdorfer, W. Molecular Spintronics Using Single-Molecule Magnets. *Nat Mater* **2008**, *7* (3), 179–186. https://doi.org/10.1038/nmat2133.

(9) Wernsdorfer, W.; Murugesu, M.; Christou, G. Resonant Tunneling in Truly Axial Symmetry Mn12Single-Molecule Magnets: Sharp Crossover between Thermally Assisted and Pure Quantum Tunneling. *Phys Rev Lett* **2006**, *96* (5), 057208. https://doi.org/10.1103/PhysRevLett.96.057208.

(10) Urdampilleta, M.; Klyatskaya, S.; Cleuziou, J. P.; Ruben, M.; Wernsdorfer, W. Supramolecular Spin Valves. *Nature Materials 2011 10:7* **2011**, *10* (7), 502–506. https://doi.org/10.1038/nmat3050.

(11) Mannini, M.; Pineider, F.; Danieli, C.; Totti, F.; Sorace, L.; Sainctavit, P.; Arrio, M. A.; Otero, E.; Joly, L.; Cezar, J. C.; Cornia, A.; Sessoli, R. Quantum Tunnelling of the Magnetization in a Monolayer of Oriented Single-Molecule Magnets. *Nature* **2010**, *468* (7322), 417–421. https://doi.org/10.1038/NATURE09478.

(12) Voss, S.; Zander, O.; Fonin, M.; Rüdiger, U.; Burgert, M.; Groth, U. Electronic Transport Properties and Orientation of Individual ${\text{Mn}}_{12}$ Single-Molecule Magnets. *Phys Rev B* **2008**, *78* (15), 155403. https://doi.org/10.1103/PhysRevB.78.155403.

(13) Saywell, A.; Magnano, G.; Satterley, C. J.; Perdigão, L. M. A.; Britton, A. J.; Taleb, N.; Del Carmen Giménez-López, M.; Champness, N. R.; O'Shea, J. N.; Beton, P. H. Self-Assembled Aggregates Formed by Single-Molecule Magnets on a Gold Surface. *Nature Communications 2010 1:1* **2010**, *1* (1), 1–8. https://doi.org/10.1038/ncomms1075.

(14) Iijima, S. Helical Microtubules of Graphitic Carbon. *Nature 1991 354:6348* **1991**, *354* (6348), 56–58. https://doi.org/10.1038/354056a0.

(15) Mintmire, J. W.; Dunlap, B. I.; White, C. T. Are Fullerene Tubules Metallic? *Phys Rev Lett* **1992**, *68* (5), 631. https://doi.org/10.1103/PhysRevLett.68.631.

(16) Iijima, S.; Ichihashi, T. Single-Shell Carbon Nanotubes of 1-Nm Diameter. *Nature* **1993**, *363* (6430), 603–605. https://doi.org/10.1038/363603a0.

(17) Ajayan, P. M.; Tsang, S. C.; Harris, P. J. F.; &green, M. L.; Hamada, N.; Sawada, S.; &oshiyama, S.; Mlntmire, J. W.; Dunlap, B. I.; &white, C. T.; Saito, R.; Fujita, F.; Dresselhaus, G.; &dresselhaus, M. S. ; D. W.; &mintmire, J. W. Cobalt-Catalysed Growth of Carbon Nanotubes with Single-Atomic-Layer Walls. *Nature 1993 363:6430* **1993**, *363* (6430), 605–607. https://doi.org/10.1038/363605a0.

(18) Kroto, H. W.; Heath, J. R.; O'Brien, S. C.; Curl, R. F.; Smalley, R. E. C60: Buckminsterfullerene. *Nature 1985 318:6042* **1985**, *318* (6042), 162–163. https://doi.org/10.1038/318162a0.

(19) Krätschmer, W.; Lamb, L. D.; Fostiropoulos, K.; Huffman, D. R. Solid C60: A New Form of Carbon. *Nature 1990 347:6291* **1990**, *347* (6291), 354–358. https://doi.org/10.1038/347354a0.

(20) *Science of Fullerenes and Carbon Nanotubes*; Elsevier, 1996. https://doi.org/10.1016/B978-0-12-221820-0.X5000-X.

(21) Terrones, M.; Grobert, N.; Zhang, J. P.; Terrones, H.; Olivares, J.; Hsu, W. K.; Hare, J. P.; Cheetham, A. K.; Kroto, H. W.; Walton, D. R. M. Preparation of Aligned Carbon Nanotubes Catalysed by Laser-Etched Cobalt Thin Films. *Chem Phys Lett* **1998**, *285* (5–6), 299–305. https://doi.org/10.1016/S0009-2614(98)00093-1.

(22) Endo, M.; Takeuchi, K.; Igarashi, S.; Kobori, K.; Shiraishi, M.; Kroto, H. W. The Production and Structure of Pyrolytic Carbon Nanotubes (PCNTs). *Journal of Physics and Chemistry of Solids* **1993**, *54* (12), 1841–1848. https://doi.org/10.1016/0022-3697(93)90297-5.

(23) Iijima, S.; Ajayan, P. M.; Ichihashi, T. Growth Model for Carbon Nanotubes. *Phys Rev Lett* **1992**, *69* (21), 3100. https://doi.org/10.1103/PhysRevLett.69.3100.

(24) Louie, S. G. Electronic Properties, Junctions, and Defects of Carbon Nanotubes. *Carbon Nanotubes* **2001**, *33*, 113–145. https://doi.org/10.1007/3-540-39947-X_6.

(25) Iijima, S.; Ajayan, P. M.; Ichihashi, T. Growth Model for Carbon Nanotubes. *Phys Rev Lett* **1992**, *69* (21), 3100. https://doi.org/10.1103/PhysRevLett.69.3100.

(26) Dravid, V. P.; Lin, X.; Wang, Y.; Wang, X. K.; Yee, A.; Ketterson, J. B.; Chang, R. P. H. Buckytubes and Derivatives: Their Growth and Implications for Buckyball Formation. *Science (1979)* **1993**, *259* (5101), 1601–1604. https://doi.org/10.1126/SCIENCE.259.5101.1601.

(27) Yue, Y.; Yuchi, D.; Guan, P.; Xu, J.; Guo, L.; Liu, J. Atomic Scale Observation of Oxygen Delivery during Silver–Oxygen Nanoparticle Catalysed Oxidation of Carbon Nanotubes. *Nature Communications 2016 7:1* **2016**, *7* (1), 1–7. https://doi.org/10.1038/ncomms12251.

(28) Tsang, S. C.; Chen, Y. K.; Harris, P. J. F.; Green, M. L. H. A Simple Chemical Method of Opening and Filling Carbon Nanotubes. *Nature 1994 372:6502* **1994**, *372* (6502), 159–162. https://doi.org/10.1038/372159a0.

(29) Lijima, S. Carbon Nanotubes. *MRS Bull* **1994**, *19* (11), 43–49. https://doi.org/10.1557/S0883769400048405/METRICS.

(30) Tersoff, J.; Ruoff, R. S. Structural Properties of a Carbon-Nanotube Crystal. *Phys Rev Lett* **1994**, *73* (5), 676. https://doi.org/10.1103/PhysRevLett.73.676.

(31) Srivastava, D.; Brenner, D. W.; Schall, J. D.; Ausman, K. D.; Yu, M. F.; Ruoff, R. S. Predictions of Enhanced Chemical Reactivity at Regions of Local Conformational Strain on Carbon Nanotubes: Kinky Chemistry. *Journal of Physical Chemistry B* **1999**, *103* (21), 4330–4337. https://doi.org/10.1021/JP990882S/ASSET/IMAGES/LARGE/JP990882SF00008.JPEG.

(32) Garrison, B. J.; Srivastava, D. Potential Energy Surfaces for Chemical Reactions at Solid Surfaces. *https://doi.org/10.1146/annurev.pc.46.100195.002105* **2003**, *46* (1), 373–396. https://doi.org/10.1146/ANNUREV.PC.46.100195.002105.

(33) Miyamoto, Y.; Rubio, A.; Cohen, M. L.; Louie, S. G. Chiral Tubules of Hexagonal BC2N. *Phys Rev B* **1994**, *50* (7), 4976–4979. https://doi.org/10.1103/PhysRevB.50.4976.

(34) Hamers, R. J. Nanotubes and Nanowires. *J Am Chem Soc* **2006**, *128* (12), 4163–4164. https://doi.org/10.1021/ja059884i.

(35) Lago, R. M.; Tsang, S. C.; Lu, K. L.; Chen, Y. K.; Green, M. L. H. Filling Carbon Nanotubes with Small Palladium Metal Crystallites: The Effect of Surface Acid Groups. *J Chem Soc Chem Commun* **1995**, No. 13, 1355–1356. https://doi.org/10.1039/C39950001355.

(36) Bower, C.; Suzuki, S.; Tanigaki, K.; Zhou, O. Synthesis and Structure of Pristine and Alkali-Metal-Intercalated Single-Walled Carbon Nanotubes. *Appl Phys A Mater Sci Process* **1998**, *67* (1), 47–52. https://doi.org/10.1007/S003390050736/METRICS.

(37) Hsu, W. K.; Terrones, M.; Hare, J. P.; Terrones, H.; Kroto, H. W.; Walton, D. R. M. Electrolytic Formation of Carbon Nanostructures. *Chem Phys Lett* **1996**, *262* (1–2), 161–166. https://doi.org/10.1016/0009-2614(96)01041-X.

(38) Hamon, M. A.; Chen, J.; Hu, H.; Chen, Y.; Itkis, M. E.; Rao, A. M.; Eklund, P. C.; Haddon, R. C. Dissolution of Single-Walled Carbon Nanotubes. *Advanced Materials* **1999**, *11* (10), 834–840. https://doi.org/10.1002/(SICI)1521-4095(199907)11:10<834::AID-ADMA834>3.0.CO;2-R.

(39) Mickelson, E. T.; Chiang, I. W.; Zimmerman, J. L.; Boul, P. J.; Lozano, J.; Liu, J.; Smalley, R. E.; Hauge, R. H.; Margrave, J. L. Solvation of Fluorinated Single-Wall Carbon Nanotubes in Alcohol Solvents. *J Phys Chem B* **1999**, *103* (21), 4318–4322. https://doi.org/10.1021/jp9845524.

(40) Mickelson, E. T.; Chiang, I. W.; Zimmerman, J. L.; Boul, P. J.; Lozano, J.; Liu, J.; Smalley, R. E.; Hauge, R. H.; Margrave, J. L. Solvation of Fluorinated Single-Wall Carbon Nanotubes in Alcohol Solvents. *Journal of Physical Chemistry B* **1999**, *103* (21), 4318–4322. https://doi.org/10.1021/JP9845524/ASSET/IMAGES/LARGE/JP9845524H00002.JPEG.

(41) Boul, P. J.; Liu, J.; Mickelson, E. T.; Huffman, C. B.; Ericson, L. M.; Chiang, I. W.; Smith, K. A.; Colbert, D. T.; Hauge, R. H.; Margrave, J. L.; Smalley, R. E. Reversible Sidewall Functionalization of Buckytubes. *Chem Phys Lett* **1999**, *310* (3–4), 367–372. https://doi.org/10.1016/S0009-2614(99)00713-7.

(42) Liu, J.; Casavant, M. J.; Cox, M.; Walters, D. A.; Boul, P.; Lu, W.; Rimberg, A. J.; Smith, K. A.; Colbert, D. T.; Smalley, R. E. Controlled Deposition of Individual Single-Walled Carbon Nanotubes on Chemically Functionalized Templates. *Chem Phys Lett* **1999**, *303* (1–2), 125–129. https://doi.org/10.1016/S0009-2614(99)00209-2.

(43) Winpenny, R. E. P. High-Nuclearity Paramagnetic 3d-Metal Complexes with Oxygen- and Nitrogen-Donor Ligands. *Adv Inorg Chem* **2001**, *52*, 1–11. https://doi.org/10.1016/S0898-8838(05)52001-4.

(44) Sessoli, R.; Gatteschi, D.; Tsai, H. L.; Hendrickson, D. N.; Schake, A. R.; Wang, S.; Vincent, J. B.; Christou, G.; Folting, K. High-Spin Molecules: [Mn12O12(O2CR)16(H2O)4]. *J Am Chem Soc* **1993**, *115* (5), 1804–1816. https://doi.org/10.1021/JA00058A027/SUPPL_FILE/JA1804.PDF.

(45) Gatteschi, D.; Sessoli, R. Quantum Tunneling of Magnetization and Related Phenomena in Molecular Materials. *Angewandte Chemie International Edition* **2003**, *42* (3), 268–297. https://doi.org/10.1002/anie.200390099.

(46) Christou, G.; Gatteschi, D.; Hendrickson, D. N.; Sessoli, R. Single-Molecule Magnets. *MRS Bull* **2000**, *25* (11), 66–71. https://doi.org/10.1557/mrs2000.226.

(47) Saywell, A.; Magnano, G.; Satterley, C. J.; Perdigão, L. M. A.; Britton, A. J.; Taleb, N.; Del Carmen Giménez-López, M.; Champness, N. R.; O'Shea, J. N.; Beton, P. H. Self-Assembled Aggregates Formed by Single-Molecule Magnets on a Gold Surface. *Nature Communications 2010 1:1* **2010**, *1* (1), 1–8. https://doi.org/10.1038/ncomms1075.

(48) Benjamin, S. C.; Ardavan, A.; Briggs, G. A. D.; Britz, D. A.; Gunlycke, D.; Jefferson, J.; Jones, M. A. G.; Leigh, D. F.; Lovett, B. W.; Khlobystov, A. N.; Lyon, S. A.; Morton, J. J. L.; Porfyrakis, K.; Sambrook, M. R.; Tyryshkin, A.

M. Towards a Fullerene-Based Quantum Computer. *Journal of Physics: Condensed Matter* **2006**, *18* (21), S867. https://doi.org/10.1088/0953-8984/18/21/S12.

(49) Bogani, L.; Sangregorio, C.; Sessoli, R.; Gatteschi, D. Molecular Engineering for Single-Chain-Magnet Behavior in a One-Dimensional Dysprosium-Nitronyl Nitroxide Compound. *Angewandte Chemie International Edition* **2005**, *44* (36), 5817–5821. https://doi.org/10.1002/anie.200500464.

(50) Del Carmen Giménez-López, M.; Moro, F.; La Torre, A.; Gómez-García, C. J.; Brown, P. D.; Van Slageren, J.; Khlobystov, A. N. Encapsulation of Single-Molecule Magnets in Carbon Nanotubes. *Nature Communications 2011 2:1* **2011**, *2* (1), 1–6. https://doi.org/10.1038/ncomms1415.

(51) Nakanishi, R.; Yatoo, M.; Katoh, K.; Breedlove, B.; Yamashita, M. Dysprosium Acetylacetonato Single-Molecule Magnet Encapsulated in Carbon Nanotubes. *Materials* **2016**, *10* (1), 7. https://doi.org/10.3390/ma10010007.

(52) Katoh, K.; Sato, J.; Nakanishi, R.; Ara, F.; Komeda, T.; Kuwahara, Y.; Saito, T.; Breedlove, B. K.; Yamashita, M. Terbium Bis-Phthalocyaninato Single-Molecule Magnet Encapsulated in a Single-Walled Carbon Nanotube. *J Mater Chem C Mater* **2021**, *9* (33), 10697–10704. https://doi.org/10.1039/D1TC01026C.

(53) Ito, S.; Nakanishi, R.; Katoh, K.; Breedlove, B. K.; Sato, T.; Li, Z.-Y.; Horii, Y.; Wakizaka, M.; Yamashita, M. Comparison between DySc Single-Molecule Magnetic Metallofullerenes Encapsulated in Single-Wall Carbon Nanotubes. *Dalton Transactions* **2022**, *51* (16), 6339–6344. https://doi.org/10.1039/D2DT00524G.